Scatterings of complex nuclei in the Glauber model

B. Abu-Ibrahim* and Y. Suzuki
Department of Physics, Niigata University, Niigata 950-2181, Japan
(Received 28 March 2000; published 21 August 2000)

A calculation of the complete Glauber amplitude is formulated with the use of an effective nucleon-target profile function. By relating the profile function to the elementary nucleon-nucleon profile function, a simple formula is derived to calculate the optical phase for nucleus-nucleus scattering. The resultant phase makes it possible to successfully reproduce much reaction cross section data at 800 MeV/nucleon. The effect of Coulomb dissociation on the optical phase is discussed. Its importance is studied in cases of the breakup of ^{6}He and ^{9}Li as well as the elastic scatterings of nuclei such as ^{12}C and ^{6}He by heavy targets.

PACS number(s): 24.10.−i, 21.10.Gv, 21.30.Fe, 25.60.−t

I. INTRODUCTION

The size of a nucleus is one of the most fundamental quantities to characterize nuclear properties. The nuclear charge radius or distribution can reliably be extracted from electron scattering, whereas the matter size or nucleon distribution is in general more difficult to obtain reliably. One of the conventional methods to determine the matter size is the measurement of a reaction cross section at energies of, e.g., several hundreds MeV/nucleon because the reaction cross section at such high energies primarily reflects the geometrical size of the nucleus [1]. Since the measurement of the interaction or reaction cross sections for unstable nuclei has now become possible with the use of secondary radioactive beams and demonstrated [2] the significant enhancement of the cross sections for nuclei near the neutron drip line, the determination of the matter size has received revived interest together with the understanding of the reaction mechanism of those unstable nuclei.

Many authors have attempted to relate the cross section of high-energy scattering to the nuclear density. See, for example, an excellent review [3] for the case of proton scattering at 1 GeV. Because of its simplicity the optical limit approximation (OLA) of the Glauber theory [4] has routinely been used as a convenient tool for the extraction of the sizes of unstable nuclei as in the case of stable nuclei. The optical phase in the OLA is given by a functional of the densities of the projectile and the target. Several authors have shown, however, that a treatment beyond the OLA is necessary for a quantitative analysis of the reaction cross sections [5–7] as well as the elastic-scattering cross sections [8,9] for loosely coupled nuclei such as halo nuclei because breakup effects are not properly accounted for in the OLA.

We have recently introduced a method to calculate the complete Glauber amplitude [10] for a proton-nucleus scattering, and subsequently attempted to extend it to a general nucleus-nucleus case [11]. In the latter case we considered nucleon-target (NT) scattering as an elementary vehicle in the Glauber theory by assuming the target as a scatterer and introduced a profile function Γ_{NT} for the NT scattering. In this formalism the various effects such as the Fermi motion, Pauli correlations [12], short-range dynamic correlations, etc., would be automatically included to some extent in the NT amplitude determined so as to fit experimental data. A similar approach was undertaken by other authors in a different context. Al-Khalili *et al.* [7] started from the NT S matrix in order to calculate the phase-shift function in the few-body approach. Others used $p+^{4}$He profile function [13,14] to calculate $p+^{12}$C, $p+^{16}$O, ^{4}He$+^{12}$C, and ^{4}He + Ca-isotope elastic differential cross sections.

In this paper we apply our method extensively to a number of heavy-ion systems including halo nuclei. The reaction cross sections and the elastic differential cross sections are calculated in different versions of approximations. We discuss the contribution of the Coulomb dissociation to the reaction cross section in order to study its importance in the reaction of the halo nuclei on a heavy target [15]. We show some examples of clean separation of the reaction cross section into the nuclear and Coulomb parts. Since a quantitative determination of the Coulomb dissociation cross section is impossible in the Glauber theory alone because of its violation of energy conservation, we have to be content with a qualitative estimate of the Coulomb contribution. We also apply the Γ_{NT} formalism to predict elastic differential cross sections at intermediate energies. The purpose here is not only to study the effectiveness of the formulation but also to obtain a simple, useful recipe to include the effects of the Coulomb dissociation and the nuclear-Coulomb interference in the elastic scattering.

In Sec. II we briefly summarize the formulation which utilizes the Γ_{NT} for the NT scattering, and present results of calculation for the reaction cross sections of various nuclei on the ^{12}C target. The densities of the nuclei are generated from microscopic multicluster model calculations [16–19]. In Sec. III we discuss how to construct the Γ_{NT} from the elementary nucleon-nucleon (NN) profile function. Here we demonstrate that the reaction cross sections of various nuclei incident on light targets such as ^{9}Be, ^{12}C, and ^{27}Al are all well reproduced to satisfactory accuracy. An extension to include the Coulomb dissociation is discussed in Sec. IV and applied to ^{6}He and ^{9}Li projectiles. The elastic differential cross sections at intermediate energies are examined in Sec. V by including the breakup effect of the projectile. A summary is drawn in Sec. VI.

*Permanent address: Department of Physics, Cairo University, Giza 12613, Egypt.

II. USE OF PHENOMENOLOGICAL NUCLEON-NUCLEUS PROFILE FUNCTION

The multiple scattering theory of Glauber is based on the eikonal approximation. In the Glauber model the scattering nucleons are frozen in their instantaneous positions during the passage of the incident particle through the nucleus. The total eikonal phase $\chi(\boldsymbol{b})$ acquired by the particle when passing through the nucleus at a fixed impact parameter $\boldsymbol{b}$ is equal to the sum of the phases from the individual nucleons (additivity phase), the latter contributing as if they were free. The nucleus-nucleus elastic-scattering amplitude (Glauber amplitude) is written as

$$F(\boldsymbol{q})=\frac{iK}{2\pi}\int d\boldsymbol{b}\, e^{i\boldsymbol{q}\cdot\boldsymbol{b}}(1-e^{i\chi(\boldsymbol{b})}), \tag{1}$$

where $\boldsymbol{K}$ is the momentum of the projectile and $\boldsymbol{q}$ is the momentum transferred from the projectile to the target. The elastic differential cross section is given by

$$\frac{d\sigma}{d\Omega}=|F(\boldsymbol{q})|^2, \tag{2}$$

and the total reaction cross section is calculated by

$$\sigma_R=\int d\boldsymbol{b}(1-|e^{i\chi(\boldsymbol{b})}|^2). \tag{3}$$

The optical phase-shift function $\chi(\boldsymbol{b})$ which plays a basic role in the Glauber theory is related to the NN scattering operator by

$$e^{i\chi(\boldsymbol{b})}=\langle\psi_0\theta_0|\prod_{i\in P}\prod_{j\in T}(1-\Gamma_{ij})|\psi_0\theta_0\rangle. \tag{4}$$

Here ψ_0 (θ_0) is the intrinsic wave function of the projectile (target), which does not depend on the center-of-mass coordinate. The profile function Γ for the NN scattering is usually parametrized in the form

$$\Gamma_{NN}(\boldsymbol{b})=\frac{1-i\alpha}{4\pi\beta}\sigma_{NN}\exp\left(-\frac{\boldsymbol{b}^2}{2\beta}\right), \tag{5}$$

where α is the ratio of the real to the imaginary part of the NN scattering amplitude in the forward direction, σ_{NN} is the total NN cross section, and β is the slope parameter of the NN elastic differential cross section. The argument of Γ_{ij} is an effective impact parameter, which is perpendicular to $\boldsymbol{K}$, between the ith and jth nucleons:

$$(\boldsymbol{r}_i-\boldsymbol{R}_P)^{\perp}-(\boldsymbol{r}_j-\boldsymbol{R}_T)^{\perp}+(\boldsymbol{R}_P-\boldsymbol{R}_T)^{\perp}=\boldsymbol{\xi}_i-\boldsymbol{\eta}_j+\boldsymbol{b}, \tag{6}$$

where $\boldsymbol{r}_i$ and $\boldsymbol{r}_j$ are the nucleon coordinates of the projectile and the target, and $\boldsymbol{R}_P$ and $\boldsymbol{R}_T$ are the corresponding center-of-mass coordinates, respectively. The inclusion of the Coulomb interaction will be considered in Secs. IV and V.

As seen in Eq. (4), we must calculate the matrix element of a many-body S-matrix operator, which is obviously fairly involved. The OLA approximation makes it possible to calculate the optical phase through the densities of the projectile and the target

$$\begin{aligned}e^{i\chi_{\mathrm{OLA}}(\boldsymbol{b})}&=\exp\left\{-\langle\psi_0\theta_0|\sum_{i\in P}\sum_{j\in T}\Gamma_{NN}(\boldsymbol{\xi}_i-\boldsymbol{\eta}_j+\boldsymbol{b})|\psi_0\theta_0\rangle\right\}\\&=\exp\left\{-\int\int d\boldsymbol{r}\,d\boldsymbol{s}\,\rho_P(\boldsymbol{r})\rho_T(\boldsymbol{s})\Gamma_{NN}(\boldsymbol{\xi}-\boldsymbol{\eta}+\boldsymbol{b})\right\}.\end{aligned} \tag{7}$$

A further simplification of OLA is possible by assuming the zero-range profile function. See, for example, [20] for the application of this approximation.

Apparently no correlated motion of the projectile and target wave functions shows up in the OLA. The use of such wave functions is certainly desirable. Some efforts were made to study corrections to the OLA [21]. They are based on including higher-order terms in the cumulant expansion [4], which is extremely involved in general. We have recently proposed an alternative method of calculating the optical phase-shift function completely [10] and applied it to the analysis of $p+{}^6$He scattering by using various types of ^{6}He wave functions. The calculation with a microscopic $\alpha+n+n$ wave function [16] has reproduced very well the angular distribution measured at 717 MeV. Owing to the power of this parameter-free, complete calculation we were led to the conclusion that the size of ^{6}He is about 2.51 fm. Though this method can straightforwardly be applied to calculate the optical phase of Eq. (4) for a general case, it would require enormous computer-time when one uses microscopic wave functions for both the projectile and the target. It is, therefore, undoubtedly necessary to further develop an effective method by which one can avoid heavy computational loads, while keeping high accuracy. This demand will be of practical significance because the reaction at high energy primarily probes the surface region of the nuclear wave function.

To this end we have proposed in [11] the possibility of using nucleon-target (NT) interaction as an elementary vehicle in the Glauber theory. The optical phase-shift function is then calculated through

$$e^{i\tilde{\chi}(\boldsymbol{b})}=\langle\psi_0|\prod_{i\in P}[1-\Gamma_{NT}(\boldsymbol{\xi}_i+\boldsymbol{b})]|\psi_0\rangle, \tag{8}$$

where Γ_{NT} may be parametrized as

$$\Gamma_{NT}(\boldsymbol{b})=\sum_{k=1}^{K}\frac{1-i\alpha_k}{4\pi\beta_k}\sigma_k\exp\left(-\frac{\boldsymbol{b}^2}{2\beta_k}\right), \tag{9}$$

and the parameters σ_k, β_k, and α_k can be determined by fitting the experimental elastic angular distribution as well as the total and reaction cross sections. The parameters of Γ_{NT} used in this paper are listed in Table I. As shown in [11] this effective theory enables us to predict both elastic differential cross sections and reaction cross sections to much better accuracy than the OLA calculation. A complete calculation of the optical phase-shift function with this Γ_{NT} can be per-

TABLE I. Parameters of proton-^{12}C profile functions used in the present calculations, see Eq. (9). The total and reaction cross sections, σ_T and σ_R, calculated by the profile functions are also shown.

T_p (MeV)	σ_T (mb)	σ_R (mb)	σ (fm^2)	β (fm^2)	α
800	341	249	52.89	1.9702	−0.111 682
			−18.78	1.0735	0.0149455
398	285	221	32.303	2.117	0.0867
			−3.740	0.5204	0.4212
340	283	213	32.0	2.0	0.1
			−3.7	0.4	0.28
200	275	215	31.947	2.214	0.127
			−4.51	0.827	0.8852

formed by the formalism presented in [10] with a slight modification as explained in the Appendix.

If we take the leading term of the cumulant expansion in the right-hand side of Eq. (8), we get a simple expression to calculate the optical phase-shift function

$$e^{i\tilde{\chi}_{\mathrm{OLA}}(\boldsymbol{b})} = \exp\left(-\int d\boldsymbol{r}\, \rho_P(\boldsymbol{r}) \Gamma_{NT}(\boldsymbol{\xi}+\boldsymbol{b}) \right), \qquad (10)$$

where we only need the density of the projectile and the Γ_{NT} of Eq. (9). This expression looks very appealing because of its simplicity. We used the $p+^{12}$C data at 800 MeV [22] to determine the Γ_{NT} parameters. A sample set of parameters given in [11] is listed in Table I. The reaction cross section calculated with $\tilde{\chi}_{\mathrm{OLA}}$ was compared in [11] to that calculated with $\tilde{\chi}$ for the ^{6}He+^{12}C case. The difference between them is only 2.6%. To examine a wide applicability of the formula (10), we have analyzed the reaction cross sections of various nuclei incident on the ^{12}C target. The densities of the nuclei ^{7}Li, ^{7}Be, ^{8}Li, ^{8}B, ^{9}Li, and ^{9}C were generated from [17], the density of ^{8}He from [18] and the density of ^{10}Be was from [19]. These densities were all obtained by the stochastic variational calculations [23,24] based on a microscopic multicluster model. See the references for detail. The accuracy of the variational calculations is generally high but differs from nucleus to nucleus depending on the complexity of the model and the consistency between the cluster model assumption and the nucleon-nucleon potential used in the calculation. For example, the calculation for ^{8}He is probably not as complete as those for other nuclei because it was performed by neglecting the spin-orbit component of the effective nucleon-nucleon potential in a five-cluster system of $\alpha+n+n+n+n$. One may use some other realistic densities, but in the present study we use our own densities obtained by the microscopic calculations because we want to test the extent to which the microscopic multicluster model produces reasonable densities. The densities obtained theoretically were first fitted by a sum of Gaussians,

TABLE II. A comparison of theoretical reaction cross sections for ^{12}C target, in units of mb, with interaction cross sections measured at 800 MeV/nucleon. The phase-shift functions are calculated by using Eqs. (7) (χ_{OLA}) and (10) ($\tilde{\chi}_{\mathrm{OLA}}$). No Coulomb interaction is included. r_m is the matter root-mean-square radius calculated by the density used in the present work. The cross section in parentheses is taken at 730 MeV/nucleon.

Projectile	r_m (fm)	σ_R		Expt. [2]
		(χ_{OLA})	($\tilde{\chi}_{\mathrm{OLA}}$)	
^{6}He	2.49	782	717	722±6
^{7}Li	2.35	789	742	736±6
^{7}Be	2.31	780	735	738±9
^{8}He	2.44	848	791	817±6
^{8}Li	2.37	824	780	768±9
^{8}B	2.38	829	783	798±6[a]
^{9}Li	2.32	841	801	796±6
^{9}Be	2.41	854	814	806±9
^{9}C	2.49	887	837	(834±18)[b]
^{10}Be	2.28	851	817	813±13
^{12}C	2.33	896	869	856±9
^{27}Al	2.88	1265	1239	

[a]Reference [25].
[b]Reference [26].

$$\rho(r) = \Sigma_i C_i \exp[-(r/a_i)^2],$$

and then corrected in the region of large r where the original densities have a Gaussian falloff. Since some of the nuclei are very weakly bound and expected to have a long tail, we assumed that the asymptotic form of the density follows a function $(a/r^2+b/r^3)\exp(-2\kappa r)$ with $\kappa^2=2\mu B/\hbar^2$, where μ is the reduced mass and B is the separation energy corresponding to the lowest accessible threshold. Values of a and b were determined to match the original density smoothly at appropriately chosen large r. The matter root-mean-square radius determined in this way may not be always the same as original theoretical one. The densities of ^{9}Be, ^{12}C, and ^{27}Al were taken from [6]. Table II lists the reaction cross sections of various projectiles incident on ^{12}C target at 800 MeV/nucleon. To fix the Γ_{NN} parameters we averaged pp and pn data [27] for the sake of simplicity: $\sigma_{NN}=43.3$ mb, $\beta=0.20$ fm^2, and $\alpha=-0.1$. These values are the same as used in [6]. The matter root-mean-square radii calculated from the above densities are also listed in the table. The cross sections calculated with Eq. (10) are compared to those obtained by usual OLA. As seen clearly, it is the simple formula of Eq. (10) that gives results closer to the measured values. There is a considerable interest in the size of ^{8}B because of its possible proton-halo structure. The density of ^{8}B used in this calculation gives 2.38 fm (2.56 fm originally [17]) for the matter root-mean-square radius, which indicates that ^{8}B is a nucleus of normal size, and the resultant cross section of 783 mb is only slightly smaller than the measured value [25] which shows no particular enhancement compared to those of the other $A=8$ isobars. The deviation from the experimental data is only within a few percent for all the

cases, which demonstrates the utility of Γ_{NT} as an elementary vehicle to analyze the high-energy nucleus-nucleus reaction. The Coulomb interaction has been neglected in fitting the $p+{}^{12}$C elastic-scattering data. In the case of a more heavy target, the NT elastic-scattering amplitude must be calculated by including the Coulomb elastic-scattering amplitude as will be discussed in Sec. IV.

We end this section by mentioning that the reaction cross section can also be calculated in the multiple-scattering theory formulation. See, for example, [27,28] for this subject.

III. RELATING Γ_{NT} TO Γ_{NN} AND ITS APPLICATION

As shown in the previous section, once Γ_{NT} is determined to fit NT scattering data at a given energy, we can systematically calculate the reactions of various projectiles incident on that target at the same incident energy per nucleon. In this way we can examine projectile wave functions. In such a case where no appropriate data are available, however, we cannot determine the Γ_{NT} and one may think that the method would not work. To overcome this difficulty, it is useful to relate the Γ_{NT} to the elementary function Γ_{NN} as described below. In any case to establish the relationship between Γ_{NT} and Γ_{NN} is important because it gives a basis for the microscopic understanding of the nucleus-nucleus collision. This important point was discussed in [3], where the NT scattering formulated in the impulse approximation is compared to that of the Glauber model.

Since the Γ_{NT} is such that its Fourier transform gives the NT elastic-scattering amplitude, we may express it in terms of Γ_{NN} by

$$\Gamma_{NT}(\boldsymbol{b})=1-\langle\theta_0|\prod_{j\in T}(1-\Gamma_{NN}(\boldsymbol{b}-\boldsymbol{\eta}_j))|\theta_0\rangle. \tag{11}$$

Equation (8) or (10) together with Eq. (11) gives us an alternative to calculate the optical phase-shift function through Γ_{NN}.

The use of the cumulant expansion leads to a very simple calculation of the optical phase-shift function. By approximating the right-hand side of Eq. (11) as

$$\Gamma_{NT}(\boldsymbol{b})\approx 1-\exp\left(-\int d\boldsymbol{s}\,\rho_T(\boldsymbol{s})\Gamma_{NN}(\boldsymbol{b}-\boldsymbol{\eta})\right) \tag{12}$$

and substituting it into Eq. (10), we obtain

$$e^{i\chi_{\rm eff}(\boldsymbol{b})}=\exp\left[-\int d\boldsymbol{r}\,\rho_P(\boldsymbol{r})\left\{1-\exp\left(-\int d\boldsymbol{s}\,\rho_T(\boldsymbol{s})\times\Gamma_{NN}(\boldsymbol{\xi}-\boldsymbol{\eta}+\boldsymbol{b})\right)\right\}\right]. \tag{13}$$

This formula is very useful because it requires only the densities of the projectile and the target. If the integral of $\rho_T\Gamma_{NN}$ is small enough compared to unity, then Eq. (13) reduces to the usual OLA formula of Eq. (7), otherwise the effect of multiple scatterings of the projectile nucleon with the target nucleons is included to some extent. To understand this point, we note that Eq. (8) may be derived by using in Eq. (4) the following approximation: That is, the operation of $\Pi_{j\in T}(1-\Gamma_{NN}(\boldsymbol{\xi}_i-\boldsymbol{\eta}_j+\boldsymbol{b}))$ on θ_0 is replaced by

$$\begin{aligned}&\prod_{j\in T}[1-\Gamma_{NN}(\boldsymbol{\xi}_i-\boldsymbol{\eta}_j+\boldsymbol{b})]|\theta_0\rangle\\ &\quad\rightarrow|\theta_0\rangle\langle\theta_0|\prod_{j\in T}[1-\Gamma_{NN}(\boldsymbol{\xi}_i-\boldsymbol{\eta}_j+\boldsymbol{b})]|\theta_0\rangle\\ &\quad=[1-\Gamma_{NT}(\boldsymbol{\xi}_i+\boldsymbol{b})]|\theta_0\rangle\end{aligned} \tag{14}$$

for any ith nucleon in the projectile. By repeating this replacement over all the projectile nucleons we arrive at Eq. (8).

Since the role of the projectile and the target is interchangeable in the calculation of the elastic-scattering amplitude as well as the reaction cross section, it may be possible to symmetrize Eq. (13) as follows:

$$e^{i\chi_{\rm effs}(\boldsymbol{b})}=\exp\left[-\frac{1}{2}\int d\boldsymbol{r}\,\rho_P(\boldsymbol{r})\left\{1-\exp\left(-\int d\boldsymbol{s}\,\rho_T(\boldsymbol{s})\times\Gamma_{NN}(\boldsymbol{\xi}-\boldsymbol{\eta}+\boldsymbol{b})\right)\right\}\right]\exp\left[-\frac{1}{2}\int d\boldsymbol{s}\,\rho_T(\boldsymbol{s})\times\left\{1-\exp\left(-\int d\boldsymbol{r}\,\rho_P(\boldsymbol{r})\Gamma_{NN}(\boldsymbol{\eta}-\boldsymbol{\xi}+\boldsymbol{b})\right)\right\}\right]. \tag{15}$$

This argument will be justified in cases where both of the nucleon-projectile and nucleon-target scatterings are well described by the densities of the projectile and the target. In cases where Γ_{NT} is unknown, Eq. (13) or (15) is expected to be a substitute to calculate the optical phase-shift function. The input data needed in the above equations are the densities and Γ_{NN}, which are exactly the same as in the usual OLA. In what follows we compare the reaction cross sections calculated with both formulas by using the same input data.

A comparison with experiment is made in Table III for reaction cross sections of different projectiles incident on different target nuclei. The densities of the targets, ^{9}Be, ^{12}C, and ^{27}Al (and also ^{63}Cu and ^{208}Pb which we need later), were taken from Table 2 of [6]. They were constructed from the simplest harmonic-oscillator shell model in which the oscillator parameter was set to reproduce the charge radius corrected by the finite size of the proton. The reaction cross sections are calculated by using three different optical phases given by Eqs. (13), (15), and (7) but by using the same densities of both the projectile and the target and the same Γ_{NN} parameters. Clearly the deviation of the theoretical cross section from experiment is by far small when using the effective Γ_{NT} compared to the one by the usual OLA. Though the deviation from the experiment depends on the quality of the density as well, it is worthwhile to note that a better prediction has been made globally with the use of Γ_{NT}. This finding is useful for extracting the nuclear size from reaction cross sections. It is agreeable that the difference in the cross

TABLE III. A comparison of theoretical reaction cross sections, in units of mb, with interaction cross sections measured at 800 MeV/nucleon. The optical phase-shift functions are calculated from the common input for the densities and Γ_{NN} in three different approximations: Eq. (7) ($\chi_{\rm OLA}$), Eq. (13) ($\chi_{\rm eff}$), and Eq. (15) ($\chi_{\rm effs}$). No Coulomb interaction is included. The cross sections in parentheses are taken at 730 MeV/nucleon. $\Delta\sigma$ denotes the deviation, given in %, from the experiment.

Target	Projectile	σ_R ($\Delta\sigma$) ($\chi_{\rm OLA}$)	($\chi_{\rm eff}$)	($\chi_{\rm effs}$)	Expt. [2]
^{9}Be	^{6}He	716 (7)	660 (2)	672 (0)	672±7
	^{7}Li	737 (7)	692 (0.9)	697 (2)	686±4
	^{7}Be	728 (7)	685 (0.4)	689 (1)	682±6
	^{8}He	788 (4)	738 (3)	744 (2)	757±4
	^{8}Li	773 (6)	730 (0.4)	733 (0.8)	727±6
	^{8}B	776 (6)	732 (0.5)	735 (0.5)	731±15
	^{9}Li	792 (7)	752 (2)	752 (2)	739±5
	^{9}Be	805 (7)	765 (1)	765 (1)	755±5
	^{9}C	830 (9)	784 (3)	788 (4)	(759±15)[a]
	^{10}Be	806(6)	769 (2)	765 (1)	755±7
^{12}C	^{6}He	782 (8)	707 (2)	732 (1)	722±6
	^{7}Li	789 (7)	734 (0.3)	748 (2)	736±6
	^{7}Be	780 (6)	726 (2)	739 (0.1)	738±9
	^{8}He	848 (4)	781 (4)	800 (2)	817±6
	^{8}Li	824 (7)	771 (0.4)	783 (2)	768±9
	^{8}B	829 (4)	772 (3)	786 (2)	798±6
	^{9}Li	841 (6)	791 (0.6)	800 (0.5)	796±6
	^{9}Be	854 (6)	804 (0.3)	813 (0.9)	806±9
	^{9}C	887 (6)	827 (0.8)	843 (1)	(834±18)[a]
	^{10}Be	851(5)	806 (1)	811 (0.3)	813±13
	^{12}C	896 (5)	856 (0)	856 (0)	856±9
^{27}Al	^{6}He	1165 (10)	1049 (1)	1096 (3)	1063±8
	^{7}Li	1143 (7)	1072 (0.1)	1094 (2)	1071±7
	^{7}Be	1132 (8)	1061 (1)	1082 (3)	1050±17
	^{8}He	1233 (3)	1137 (5)	1171 (2)	1197±9
	^{8}Li	1185 (3)	1116 (3)	1135 (1)	1147±14
	^{8}B	1193 (8)	1119 (1)	1141 (3)	1106±32
	^{9}Li	1204 (6)	1140 (0.4)	1155 (2)	1135±7
	^{9}Be	1218 (4)	1156 (2)	1170 (0.3)	1174±10
	^{9}C	1265 (7)	1186 (0.4)	1212 (3)	(1181±29)[a]
	^{10}Be	1215(5)	1156(0.3)	1166 (1)	1153±16
	^{12}C	1265	1217	1219	

[a]Reference [26].

sections obtained with Eqs. (13) and (15) is found to be very small. By comparing the σ_R values for ^{12}C target in Tables II and III, we note that the symmetrized optical phase-shift function of Eq. (15) predicts almost the same values as that of Eq. (10). Figure 1 compares three different $\chi(\boldsymbol{b})$ as defined by Eqs. (8), (15), and (7) for ^{6}He+^{12}C scattering at 800 MeV/nucleon. The solid curve is calculated by Eq. (8) with the use of a microscopic ^{6}He wave function [16] and used to predict the elastic differential cross section of ^{6}He+^{12}C scattering [11]. Therefore, the solid curve is obtained without any approximations and may be considered the reference phase. Since the breakup probability is given by $1-\exp(-2\,\mathrm{Im}\,\chi(\boldsymbol{b}))$ as a function of b, we understand that the dashed curve calculated by Eq. (15) gives the reaction cross section much closer to the reference one than that by the usual OLA.

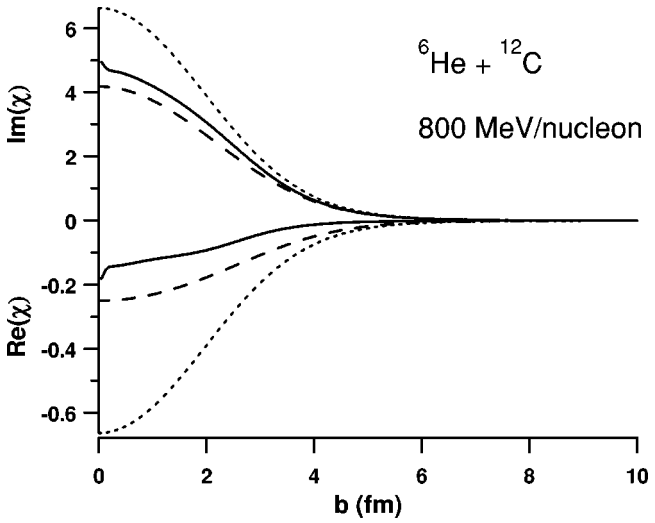

FIG. 1. A comparison of both real and imaginary parts of the optical phases for ^{6}He+^{12}C scattering at 800 MeV/nucleon as a function of the impact parameter b: the solid curve is from Eq. (8) ($\tilde{\chi}$) with the use of a microscopic ^{6}He wave function [16], the dashed curve is from Eq. (15) ($\chi_{\rm eff}$), and the dotted curve from Eq. (7) ($\chi_{\rm OLA}$).

We end this section by showing $p+^{12}$C elastic differential cross sections calculated by the theoretical profile function of Eq. (12) and comparing them with experiment [22,29,30]. This will be useful to indicate the medium effect or Pauli correlations [3,12] which may be important in the elementary NT interaction. Figure 2 displays the cross sections at three different energies. The solid curve is the phenomenological fit by Eq. (9), whose parameters are listed in Table I, while the dashed one is the OLA prediction of Eq. (12). Parameters of Γ_{NN} are taken from [27]. It is seen that the OLA calculation produces a very reasonable fit to experiment at $T_p=800$ MeV [22]. Particularly, the fit is very satisfactory up to about 15 degrees. This is probably the reason why the effective optical phases, $\chi_{\rm eff}$ and $\chi_{\rm effs}$, lead to a good reproduction of the reaction cross sections at 800 MeV/nucleon. The OLA is still fairly good at $T_p=400$ MeV. As the energy decreases to $T_p=300$-200 MeV, the σ_{NN} value reaches its minimum and the nuclear transparency increases. We may expect a larger medium effect at this energy. In fact we see in the figure that the OLA phase [Eq. (12)] does not reproduce the experimental data [29,30] even at forward angles.

IV. EFFECTS OF COULOMB DISSOCIATION

When it passes by a large-Z target with high velocity, a projectile nucleus receives a rapidly changing electromag-

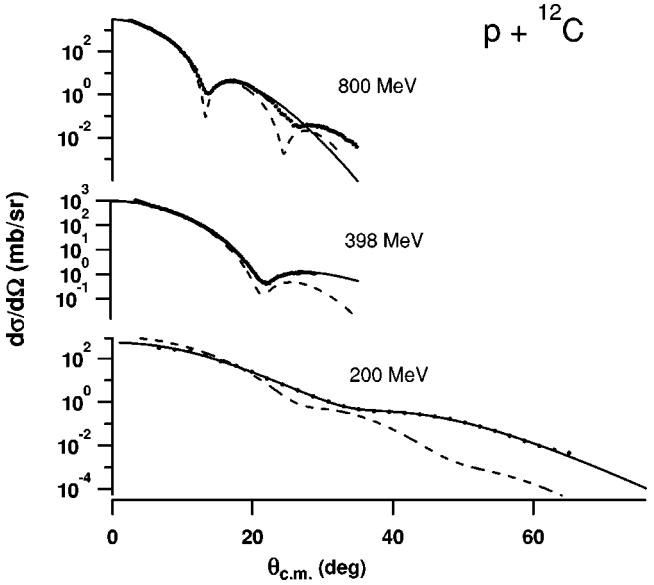

FIG. 2. $p+{}^{12}$C elastic differential cross sections at three different energies. The solid curve is a phenomenological fit of Eq. (9), while the dashed curve is the OLA prediction of Eq. (12). The data are taken from [22,29,30].

netic field created by the target nucleus and thus may be excited by the field when the impact parameter is greater than the nuclear interaction radius. In fact strong enhancement of the interaction cross section as well as the two-neutron removal cross section has been observed for nuclei near the drip line, a typical example of which is ^{11}Li $+{}^{208}$Pb reaction [15]. The cross section for $2n$ removal of ^{11}Li by ^{208}Pb is also extremely large compared with the case observed for stable nuclei [31]. The enhancement of the Coulomb dissociation cross section may be related to the strength of electric multipole, particularly the electric dipole at low excitation energy of unstable nuclei. The aim of this section is an attempt to estimate the contribution of the Coulomb dissociation to the reaction cross section in the Glauber theory. Some works have been directed to this subject in the Glauber model [32,33] following the formalism of deuteron breakup by heavy targets. We must admit, however, that this aim is limited by the fact that the direct use of the Glauber theory leads to an unphysical result at large impact parameter because of the violation of energy conservation which is inherent in the Glauber theory. This remark applies at large b where the Coulomb force becomes weak but still has the possibility of exciting a very weakly binding halo nucleus. What we can do is to estimate qualitatively the Coulomb dissociation cross section as a function of b by assuming that there is a region of b where the adiabatic approach of the Glauber theory is applicable. The violation of energy conservation would be a serious problem in cases where most of the electric dipole strength is concentrated in the high-energy giant resonance region as in normal nuclei.

Using the phase additivity concept, we can write the elastic-scattering amplitude, Eq. (1), with the Coulomb interaction being included in the form

$$F(\boldsymbol{q})=\frac{iK}{2\pi}\int d\boldsymbol{b}\, e^{i\boldsymbol{q}\cdot\boldsymbol{b}}\Bigg[1-\langle\psi_0|\exp\Bigg\{i\sum_{i=1}^{A_P}\chi_{NT}(\boldsymbol{\xi}_i+\boldsymbol{b}) +i\sum_{i=1}^{Z_P}\chi_C(\boldsymbol{\xi}_i+\boldsymbol{b})\Bigg\}|\psi_0\rangle\Bigg]$$
$$=\frac{iK}{2\pi}\int d\boldsymbol{b}e^{i\boldsymbol{q}\cdot\boldsymbol{b}}\{1-e^{iZ_P\chi_C(b)}+e^{iZ_P\chi_C(b)}(1-e^{i\tilde{\chi}_t(\boldsymbol{b})})\}$$
$$=F_C(q)+\frac{iK}{2\pi}\int d\boldsymbol{b}\, e^{i\boldsymbol{q}\cdot\boldsymbol{b}+iZ_P\chi_C(b)}(1-e^{i\tilde{\chi}_t(\boldsymbol{b})}), \qquad (16)$$

where $\exp(i\chi_{NT})=1-\Gamma_{NT}$ is the nuclear phase-shift function for NT scattering, which was discussed in the previous sections and the Coulomb phase is given by $\chi_C(b)=2\eta\ln(Kb)$ with the Sommerfeld parameter $\eta=Z_Te^2/\hbar v$, where v is the velocity of the projectile. $F_C(q)$ is the Coulomb elastic-scattering amplitude which produces the Rutherford formula. Note that the target is considered as a charged point-particle. The total optical phase $\tilde{\chi}_t(\boldsymbol{b})$ with the effect of the Coulomb dissociation being included is defined by

$$e^{i\tilde{\chi}_t(\boldsymbol{b})}=\langle\psi_0|\exp\Bigg[i\sum_{i=1}^{A_P}\chi_{NT}(\boldsymbol{\xi}_i+\boldsymbol{b}) +i\sum_{i=1}^{Z_P}\{\chi_C(\boldsymbol{\xi}_i+\boldsymbol{b})-\chi_C(b)\}\Bigg]|\psi_0\rangle$$
$$=\langle\psi_0|\exp\Bigg[i\sum_{i=1}^{A_P}\{\chi_{NT}(\boldsymbol{\xi}_i+\boldsymbol{b})+\epsilon_i\Delta\chi_C(\boldsymbol{\xi}_i+\boldsymbol{b})\}\Bigg]|\psi_0\rangle, \qquad (17)$$

where

$$\Delta\chi_C(\boldsymbol{\xi}+\boldsymbol{b})=2\eta\ln\left(\frac{|\boldsymbol{\xi}+\boldsymbol{b}|}{b}\right), \quad \epsilon_i=\begin{cases}1 & i\in\text{proton},\\ 0 & i\in\text{neutron}.\end{cases} \qquad (18)$$

By writing $\exp(i\Delta\chi_C)=1-\Gamma_C$ with

$$\Gamma_C(\boldsymbol{\xi}+\boldsymbol{b})=1-\left(\frac{|\boldsymbol{\xi}+\boldsymbol{b}|}{b}\right)^{2i\eta}, \qquad (19)$$

Eq. (17) can be expressed in terms of the NT profile function Γ_t which enables us to examine the effect of the Coulomb dissociation:

$$e^{i\tilde{\chi}_t(\boldsymbol{b})}=\langle\psi_0|\prod_{i\in P}[1-\Gamma_t(\boldsymbol{\xi}_i+\boldsymbol{b})]|\psi_0\rangle \qquad (20)$$

with

$$1-\Gamma_t(\boldsymbol{\xi}_i+\boldsymbol{b})=[1-\Gamma_{NT}(\boldsymbol{\xi}_i+\boldsymbol{b})][1-\epsilon_i\Gamma_C(\boldsymbol{\xi}_i+\boldsymbol{b})]. \qquad (21)$$

In the approximation of taking the leading term of the cumulant expansion in Eq. (20) we can extend the formula of Eq. (10) so as to include the Coulomb dissociation term:

$$e^{i\tilde{\chi}_t(\boldsymbol{b})} \approx \exp[i\gamma_N(\boldsymbol{b}) + i\gamma_C(\boldsymbol{b}) + i\gamma_{NC}(\boldsymbol{b})], \tag{22}$$

where the nuclear, Coulomb, and nuclear-Coulomb interference phases are, respectively, defined by

$$i\gamma_N(\boldsymbol{b}) = -\int d\boldsymbol{r}\,\rho_P(\boldsymbol{r})\Gamma_{NT}(\boldsymbol{\xi}+\boldsymbol{b}) = i\tilde{\chi}_{\mathrm{OLA}}(\boldsymbol{b}),$$

$$i\gamma_C(\boldsymbol{b}) = -\int d\boldsymbol{r}\,\rho_P^{(C)}(\boldsymbol{r})\Gamma_C(\boldsymbol{\xi}+\boldsymbol{b}),$$

$$i\gamma_{NC}(\boldsymbol{b}) = \int d\boldsymbol{r}\,\rho_P^{(C)}(\boldsymbol{r})\Gamma_{NT}(\boldsymbol{\xi}+\boldsymbol{b})\Gamma_C(\boldsymbol{\xi}+\boldsymbol{b}). \tag{23}$$

Here $\rho_P(\boldsymbol{r})$ is the nucleon density of the projectile as defined before, whereas $\rho_P^{(C)}(\boldsymbol{r})$ is the charge density of the projectile. In this approximation the nuclear part of the total optical phase is the same as given by Eq. (10). The phase γ_N may be replaced by $\tilde{\chi}$ of Eq. (8) or χ_{eff} of Eq. (13).

By replacing $|e^{i\chi(\boldsymbol{b})}|^2$ in Eq. (3) with $|e^{iZ_P\chi_C(\boldsymbol{b})}e^{i\tilde{\chi}_t(\boldsymbol{b})}|^2 = |e^{i\tilde{\chi}_t(\boldsymbol{b})}|^2$ we obtain the reaction cross section. With the use of the identity

$$1-|e^{i\tilde{\chi}_t(\boldsymbol{b})}|^2 = (1-|e^{i\gamma_N(\boldsymbol{b})}|^2) + |e^{i\gamma_N(\boldsymbol{b})}|^2(1-|e^{i\gamma_C(\boldsymbol{b})}|^2) + |e^{i\gamma_N(\boldsymbol{b})+i\gamma_C(\boldsymbol{b})}|^2(1-|e^{i\gamma_{NC}(\boldsymbol{b})}|^2), \tag{24}$$

the reaction cross section can be decomposed into three parts:

$$\sigma_R = \sigma_R^{(N)} + \sigma_R^{(C)} + \sigma_R^{(NC)}, \tag{25}$$

where, for example, the Coulomb term $\sigma_R^{(C)}$ is given by

$$\sigma_R^{(C)} = \int d\boldsymbol{b}|e^{i\gamma_N(\boldsymbol{b})}|^2(1-|e^{i\gamma_C(\boldsymbol{b})}|^2). \tag{26}$$

This decomposition may not be unique, but seems to be physically reasonable [32,33]. Since the effective range of Γ_{NT} is limited by the nuclear interaction, both γ_N and γ_{NC} vanish at b larger than the nuclear interaction radius. The nuclear term $\sigma_R^{(N)}$ has a contribution from relatively small b where the nuclear interaction plays a vital role, while the Coulomb term is mainly contributed from larger b where the nuclear interaction becomes negligible. Taking an example of ^{6}He+^{208}Pb we display in Fig. 3 the integrand (i.e., breakup probability) contributing to the three components of $\sigma_R^{(N)}$, $\sigma_R^{(C)}$, and $\sigma_R^{(NC)}$ as a function of b. As expected, the nuclear breakup is confined in the region of the nuclear interaction radius, while the Coulomb dissociation begins to rise at such an impact parameter that is equal to the sum of the projectile and target radii. In addition, the interference term is very small everywhere. This means that the total reaction cross section is, by the decomposition (24), well separated into two terms, the nuclear cross section and the Coulomb cross section. In cases where we can predict $\sigma_R^{(N)}$ fairly accurately as shown in the previous section, this clean separation makes it possible to extract the amount of the Coulomb dissociation cross section by subtracting $\sigma_R^{(N)}$ from the measured reaction cross section. We note, however, that the isolation of the nuclear part from the total reaction cross section may become difficult when both of the projectile and target nuclei are heavy. Another interesting point in the figure is the behavior of the Coulomb integrand at large b. To understand this behavior, we note that at large b

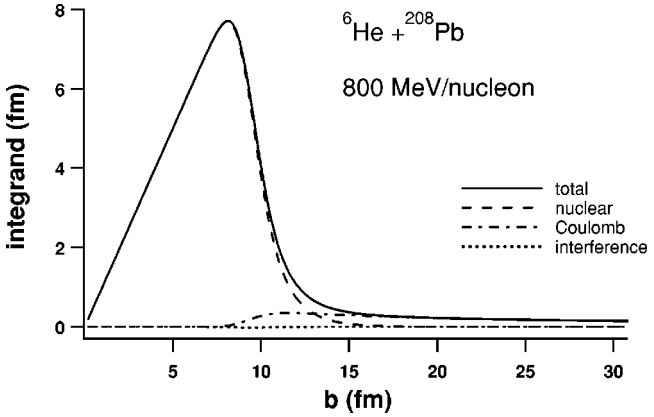

FIG. 3. Breakup probabilities, multiplied by the impact parameter b, for ^{6}He+^{208}Pb collision at 800 MeV/nucleon. The total probability is decomposed into the nuclear, Coulomb, and nuclear-Coulomb interference terms.

$$\Gamma_C(\boldsymbol{\xi}+\boldsymbol{b}) \to -\frac{2i\eta}{b}(\boldsymbol{\xi}\cdot\hat{\boldsymbol{b}}) - \frac{i\eta}{b^2}\{\xi^2 - 2(\boldsymbol{\xi}\cdot\hat{\boldsymbol{b}})^2\} + \frac{2\eta^2}{b^2}(\boldsymbol{\xi}\cdot\hat{\boldsymbol{b}})^2 + \cdots, \tag{27}$$

where $\hat{\boldsymbol{b}}$ is a unit vector defined by $\boldsymbol{b}/b$. Thus for a spherically symmetric charge density $i\gamma_C(\boldsymbol{b})$ is approximated in the order of $1/b^4$ by

$$\begin{aligned} i\gamma_C(\boldsymbol{b}) &\to -\frac{\eta^2}{b^2}\int d\boldsymbol{r}\rho_P^{(C)}(\boldsymbol{r})\xi^2 + \frac{\eta^2}{4b^4}(\eta^2 - 1 + 2i\eta) \\ &\quad \times \int d\boldsymbol{r}\,\rho_P^{(C)}(\boldsymbol{r})\xi^4 \\ &= -\frac{8\pi\eta^2}{3b^2}\int_0^\infty dr\, r^4\rho_P^{(C)}(r) + \frac{8\pi\eta^2}{15b^4}(\eta^2 - 1 \\ &\quad + 2i\eta)\int_0^\infty dr\, r^6\rho_P^{(C)}(r). \end{aligned} \tag{28}$$

The probability of the Coulomb dissociation, $(1-|e^{i\gamma_C(\boldsymbol{b})}|^2)$, is then proportional to $1/b^2$, so that the integrand for $\sigma_R^{(C)}$ has the dependence of $1/b$ as confirmed from the figure, leading to a logarithmic divergence of $\sigma_R^{(C)}$. As mentioned above, this unphysical result is due to the neglect of the energy conservation in the Glauber theory. In reality the probability of the Coulomb dissociation will decrease exponentially at large b.

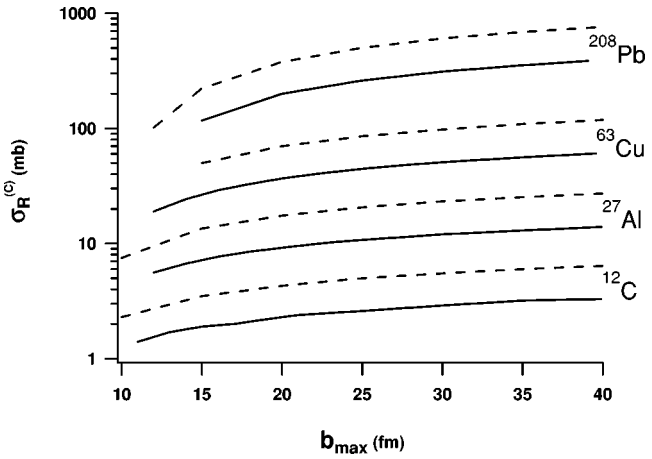

FIG. 4. Coulomb dissociation cross sections of ^{6}He and ^{9}Li incident on various targets at 800 MeV/nucleon. The solid curve is for ^{6}He and the dashed one is for ^{9}Li. The value of $b_{\max}$ is the upper limit in the integral of Eq. (26).

To get a qualitative estimate of the Coulomb dissociation cross section, we have to set an upper limit of the impact parameter, $b_{\max}$. To this end we compare the time scale required for the internal excitation of the projectile and the time scale of the collision. The former is given by $\hbar/B$ with the separation energy B, while the latter is b/v during which the electric field in the perpendicular direction to the incident velocity becomes large [34]. The latter time scale must be smaller than the former in order for the adiabaticity of the Glauber theory to be satisfied. Thus we may require the condition

$$b_{\max} < \frac{\hbar v}{B}. \tag{29}$$

This condition is also obtained by requiring that the minimum momentum transfer $\hbar q_{\min}$ needed for the Coulomb dissociation must satisfy $\hbar q_{\min} > B/v$ [35,32], because, from the uncertainty principle of the angular momentum l and the angle θ, we have $l\theta = (\hbar K b)(q/K) = \hbar b q \geqslant \hbar$, that is $\hbar q_{\min} \geqslant \hbar/b_{\max} > B/v$. As is clear from the above discussion, the condition (29) does not introduce any charge dependence on $b_{\max}$, which may be thought strange. You may think, instead, that $b_{\max}$ can be obtained by requiring that the energy transferred to the projectile by the electric field must be larger than B. If the energy transfer is estimated by taking the difference of the energy given to the projectile as a whole and the energy given to the freely moving protons [34], you may get the condition $b_{\max} < \sqrt{(2Z_P N_P/A_P)(\hbar^2/MB)}\,\eta$ [36], where M is the nucleon mass. This expression, however, cannot be accepted in the present case: For example, in the case of ^{6}He+^{208}Pb collision at 800 MeV/nucleon ($B = 0.975$ MeV), we would have $b_{\max} < 8$ fm, which means that $b_{\max}$ would be even smaller than the sum of the radii of ^{6}He and ^{208}Pb.

Figure 4 displays the Coulomb dissociation cross section $\sigma_R^{(C)}$ as a function of $b_{\max}$ for the reactions of ^{6}He and ^{9}Li projectiles incident on different target nuclei at 800 MeV/nucleon. In Table IV the measured reaction cross sections [15] are compared to the theoretical cross sections calculated by assuming $b_{\max} = (\hbar v/2B)$ as a qualitative guide. B is 4.063 MeV for ^{9}Li case, so that $b_{\max}$ becomes about a quarter of that for ^{6}He case. We see that the increase of $\sigma_R^{(C)}$ for heavier targets is a little slower than the Z_T^2 dependence. The total reaction cross section for ^{208}Pb target seems to be slightly overestimated in both cases of ^{6}He and ^{9}Li. This may suggest that the adiabatic approach based on the Glauber theory is applicable up to such $b_{\max}$ that is smaller than $(\hbar v/2B)$, and beyond that $b_{\max}$ a perturbative approach fulfilling the energy conservation must be employed.

TABLE IV. A decomposition of reaction cross sections at 800 MeV/nucleon into the nuclear (N), Coulomb (C), and nuclear-Coulomb interference (NC) terms. The cross section is given in units of mb. Values of $\sigma_R^{(C)}$ depend on $b_{\max}$, which is set to 85 fm for ^{6}He and 20 fm for ^{9}Li, respectively. The cross sections in parentheses are obtained by reducing $b_{\max}$ to 43 fm.

Projectile	Target	$\sigma_R^{(N)}$	$\sigma_R^{(NC)}$	$\sigma_R^{(C)}$	σ_R	Expt. [2,15]
^{6}He	^{12}C	707	0.09	4(3)	711(710)	722 ± 6
	^{27}Al	1049	0.05	19(14)	1068(1063)	1063 ± 8
	^{63}Cu	1676	-0.3	87(62)	1762(1737)	1747 ± 72
	^{208}Pb	3095	-4	602(406)	3693(3497)	3472 ± 251
^{9}Li	^{12}C	791	0.01	4	795	796 ± 6
	^{27}Al	1140	0.09	17	1158	1135 ± 7
	^{63}Cu	1783	-0.4	70	1852	1796 ± 55
	^{208}Pb	3228	-5	379	3603	3397 ± 193

V. ELASTIC DIFFERENTIAL CROSS SECTIONS

Elastic and inelastic scatterings at intermediate energies have been analyzed for various systems in the OLA calculation. See, for example, [37]. Main interest in these studies was to incorporate the deviation from the straight-line trajectory of the projectile, which becomes important in the case of relatively low-energy scatterings by large-Z targets. A simple prescription of including the deviation from the straight-line trajectory is to use the distance of the closest approach b'

$$b' = \frac{Z_P \eta}{K} + \sqrt{\left(\frac{Z_P \eta}{K}\right)^2 + b^2} \tag{30}$$

in Rutherford orbit in place of the asymptotic impact parameter b [37]. Our main interest here lies in evaluating the merit of using the Γ_{NT} formalism and learning the effect of the Coulomb dissociation in the elastic scattering. The effect of the Coulomb dissociation is of course different from that of the bending of the Rutherford orbit. To the best of our knowledge, no calculation of elastic scatterings with the inclusion of the Coulomb dissociation has been performed yet in the framework of the Glauber theory.

We apply the method of calculation of the optical phase to predict elastic differential cross sections between nuclei

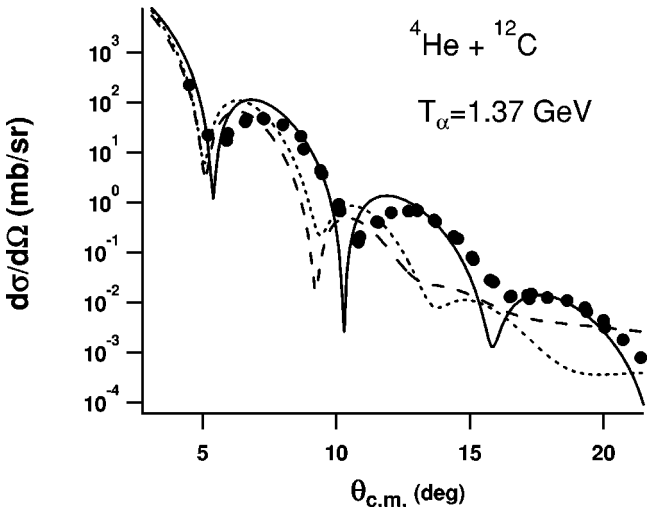

FIG. 5. Elastic differential cross sections for ^{4}He+^{12}C scattering at $T_\alpha = 1.37$ GeV. The optical phases are calculated in three ways: the solid curve from Eq. (8) ($\tilde{\chi}$) with the use of the $(0s)^4$ harmonic-oscillator shell-model wave function, the dashed curve from Eq. (13) ($\chi_{\rm eff}$), and the dotted curve from Eq. (7) ($\chi_{\rm OLA}$). The data are taken from [38].

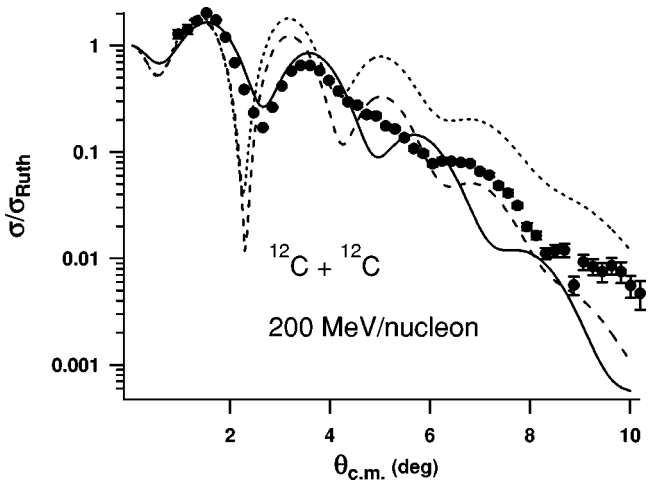

FIG. 6. Elastic differential cross sections in Rutherford ratio for ^{12}C+^{12}C scattering at 200 MeV/nucleon. The optical phases are calculated in three ways: the solid curve from Eq. (10) ($\tilde{\chi}_{\rm OLA}$), the dashed curve from Eq. (13) ($\chi_{\rm eff}$), and the dotted curve from Eq. (7) ($\chi_{\rm OLA}$). The data are taken from [39].

through the scattering amplitude, Eq. (16). The Rutherford amplitude F_C is included in what follows. The total optical phase $\tilde{\chi}_l(\boldsymbol{b})$ defined by Eqs. (20) is approximately calculated by Eqs. (22) and (23), but the nuclear part γ_N may be replaced by other approximations.

The first example, shown in Fig. 5, is ^{4}He+^{12}C scattering at the intermediate energy of $T_\alpha = 1.37$ GeV [38]. A theoretical description of this scattering was studied in [21], where terms up to the fourth order in the cumulant expansion were included. They reproduced the experiment rather well though the slope parameter β of Γ_{NN} is unusually small considering from the systematics of [27]. They found that the amplitude F_C plays a significant role even in this light system. Since no $p+^{12}$C elastic scattering data at $T_p = 343$ MeV are available, the Γ_{NT} parameters were determined by extrapolating the experimental data measured at 398 MeV [29], as discussed in [11]. The resultant parameters of Γ_{NT} are listed in Table I. The Coulomb dissociation has been neglected. The nuclear optical phase $\tilde{\chi}$ defined by Eq. (8) has been calculated by using the $(0s)^4$ harmonic-oscillator shell-model wave function [11]. Despite this unsatisfactory determination of Γ_{NT} the calculated cross section denoted by solid curve is in fair agreement with experiment, even better than the phenomenological fit of [14]. The dashed and dotted curves are obtained by replacing the nuclear optical phase $\tilde{\chi}$ by $\chi_{\rm eff}$ of Eq. (13) and by $\chi_{\rm OLA}$ of Eq. (7), respectively. The quality of fit to experiment by these phases is related to that of the underlying $p+^{12}$C elastic scattering at the same energy by the OLA (see Fig. 2).

The next example is ^{12}C+^{12}C scattering at 200 MeV/nucleon, where the total NN cross section σ_{NN} becomes about 30 mb, close to its minimum. This small cross section leads to the increase of the nuclear transparency at this energy. The angular distributions calculated with three different optical phases are displayed in Fig. 6 and compared with the experimental data [39]. The solid curve is obtained with the use of $\tilde{\chi}_{\rm OLA}$ of Eq. (10). It gives quite reasonable cross sections (better than other calculations [37,40]), and follows nicely the data at small angles up to the second peak where both of the far-side and near-side amplitudes [41] contribute to producing the oscillatory behavior [39]. At larger angles where the far-side amplitude dominates the solid curve gives the distribution which is out of phase from the experiment. The angular distributions calculated by $\chi_{\rm eff}$ and $\chi_{\rm OLA}$ are also shown in the figure. The result with $\chi_{\rm eff}$ is better than the one with $\chi_{\rm OLA}$. Figure 7 compares the reaction (absorption) probability, $1-|e^{i\chi(\boldsymbol{b})}|^2$, as a function of b'. Compared

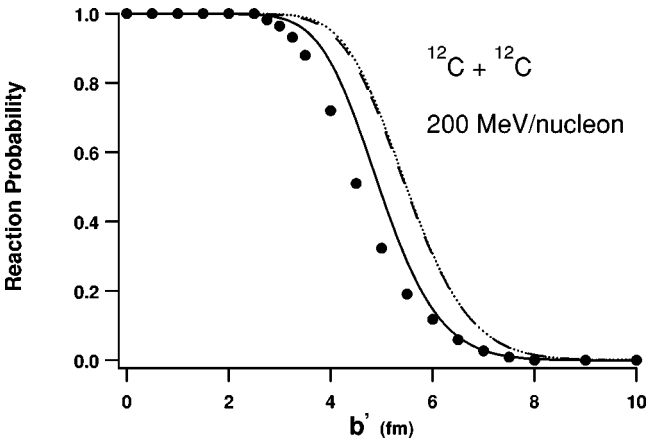

FIG. 7. Reaction probability for the ^{12}C+^{12}C collision at 200 MeV/nucleon as a function of the distance of the closest approach b'. The optical phases are calculated in three ways: the solid curve from Eq. (10) ($\tilde{\chi}_{\rm OLA}$), the dashed curve from Eq. (13) ($\chi_{\rm eff}$), and the dotted curve from Eq. (7) ($\chi_{\rm OLA}$). The black circle is the optical-model prediction [39].

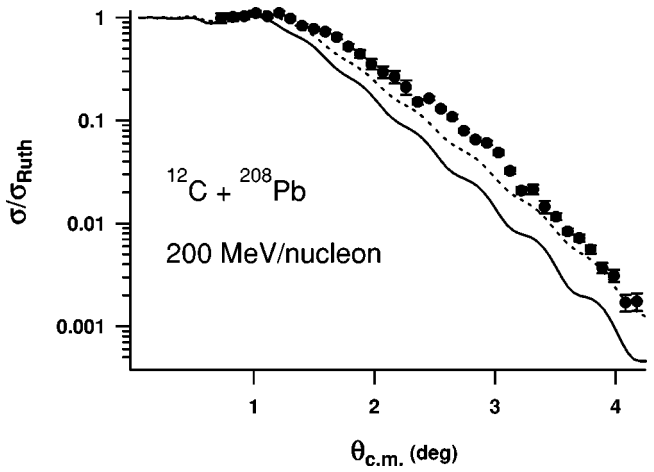

FIG. 8. Elastic differential cross sections in the Rutherford ratio for $^{12}C+^{208}Pb$ scattering at 200 MeV/nucleon. The dotted curve: only the nuclear term calculated by Eq. (13) ($\chi_{\rm eff}$) is included, the solid curve: both nuclear and Coulomb terms are included. The data are taken from [39].

to the reaction probability calculated from the optical potential [39] which is determined by fitting the elastic angular distribution, our theoretical curves suggest too strong an absorption: The curve calculated with $\tilde{\chi}_{\rm OLA}$ is, however, fairly close to the optical-model prediction. Corresponding to the three different reaction probabilities, the $^{12}C+^{12}C$ reaction cross sections at 200 MeV/nucleon are calculated to be, respectively, 817 ($\tilde{\chi}_{\rm OLA}$), 994 ($\chi_{\rm eff}$), and 1002 mb ($\chi_{\rm OLA}$), which are compared to the measured value of 864 ± 45 mb [42] or the value of 806 ± 30 mb predicted by the optical potential [39]. We see that the optical phase $\tilde{\chi}_{\rm OLA}$ gives such a reaction cross section, which is consistent with experiment, nevertheless it leads to some discrepancy in the elastic angular distribution at large angles. This may indicate that we must take into account the coupling to excited states of ^{12}C explicitly or some unknown medium effects.

Figure 8 displays $^{12}C+^{208}Pb$ scattering at 200 MeV/nucleon. The Coulomb repulsion becomes as large as about 70 MeV at the internuclear distance of 10 fm. In the range of measured angles the near-side contribution is dominant [39] because the net effect of the nuclear and Coulomb potentials is largely repulsive. Since there are no data on $p+^{208}Pb$ at $T_p=200$ MeV, the nuclear optical phase has been calculated through $\chi_{\rm eff}$ of Eq. (13). As far as we know, this is a microscopic calculation for $^{12}C+^{208}Pb$ scattering for the first time in which the Γ_{NN} data and the densities of the projectile and target are employed. We have successively included the effects of the Coulomb dissociation and the nuclear-Coulomb interference terms. The cross sections calculated by including these effects are apparently smaller than the measured values. The bending of the Rutherford orbit plays a minor role at this energy. As the nuclear transparency is fairly large in the collision at 200 MeV/nucleon, the ^{12}C nucleus may come relatively close to the interior of the ^{208}Pb target, and then the NN collision may be Pauli-blocked fairly strongly [12]. In any case it would be necessary to use such a nuclear optical phase that reproduces the $p+^{208}Pb$ scattering at this energy before we attempt to understand the reason for this discrepancy.

VI. SUMMARY

The idea of utilizing the nucleon-target (NT) interaction as an elementary vehicle in the Glauber theory [11] has extensively been applied to calculate the nucleus-nucleus optical phase-shift function. With the use of phenomenologically determined NT profile functions, the total reaction cross section has better been reproduced than by the conventional optical limit approximation. A further simpler expression for the optical phase has been derived by relating the NT profile function to the nucleon-nucleon data. The resultant optical phase for the nucleus-nucleus scattering is given by a functional of the nuclear densities as well as the elementary nucleon-nucleon input. This simplicity has made it possible to analyze many existing data and led to the conclusion that this effective formula reproduces the reaction cross section at 800 MeV/nucleon to much better accuracy than the conventional theory.

The effect of the Coulomb dissociation on the optical phase has been discussed. It has been shown for light projectiles such as ^{6}He and ^{9}Li that the breakup probability can be very well separated into the nuclear and Coulomb parts: The nuclear-Coulomb interference term is found to be very small at the energy of 800 MeV/nucleon. Because of the difficulty inherent in the Glauber theory a definitive determination of the Coulomb dissociation cross section is impossible. The qualitative estimate of the cross section made for different targets, however, is found to lead to reasonable correspondence with experiment.

The elastic differential cross sections at intermediate energies have been calculated for some systems. The Coulomb dissociation and nuclear-Coulomb interference terms are included in the Glauber amplitude together with the bending of the Rutherford orbit. Both of the real and imaginary parts of the optical phase contribute to the cross section, so that we have more opportunities to learn the suitability of the Γ_{NT} in the analysis of the elastic differential cross section than that of the reaction cross section. Though the Glauber model prediction seems to be reasonable, we feel that more careful study is needed on the relationship between the elementary NT scattering amplitudes in free space and in nuclear medium before we attempt a better microscopic understanding of the reaction dynamics. For this purpose it would be important to perform systematic analyses of both nucleon-nucleus and nucleus-nucleus scatterings by the same target at different energies.

ACKNOWLEDGMENTS

This work was in part supported by a Grant-in-Aid for Scientific Research (No. 10640255) of the Ministry of Education, Science, Sports and Culture (Japan). B.A. thanks the Egyptian Ministry of Education for support through Scientific Channel. He is also grateful to Professor M. M. Sherif and Dr. O. M. Osman for their encouragement.

APPENDIX

The optical phase-shift function defined by Eq. (8) can be calculated by following the correlated Gaussian approach presented in [10]. Since the Γ_{NT} is given in terms of a combination of several terms as in Eq. (9), a slight modification is necessary to define the parameters of the correlated Gaussian. According to [10] we can express the phase-shift function in terms of the matrix element of the correlated Gaussian g:

$$e^{i\tilde{\chi}(\boldsymbol{b})}=1+\sum_{n=1}^{A_P}(-1)^n\sum_{(i_1,i_2,\ldots,i_n)}\sum_{k_1=1}^{K}\cdots\sum_{k_n=1}^{K}z_{k_1}\cdots z_{k_n}e^{-\Lambda\boldsymbol{b}^2}\langle\psi_0|g(u\boldsymbol{b};B,\boldsymbol{r}^{\perp})|\psi_0\rangle, \tag{A1}$$

where A_P is the number of nucleons of the projectile nucleus, and z_{k_m} stands for $\sigma_{k_m}(1-i\alpha_{k_m})/4\pi\beta_{k_m}$. The sum over $(i_1,i_2,\ldots,i_n)$ indicates a number n of different nucleons in the projectile which come into the interaction with the target. For example, in the case of $n=2$ the sum (i_1,i_2) extends over (1,2),(1,3), . . . ,(1,A_P),(2,3), . . . ,(2,A_P), . . . ,(A_{P-1},A_P). The terms with $n>1$ represent multiple scatterings of the projectile nucleons with the target. The function g is defined by

$$g(u\boldsymbol{b};B,\boldsymbol{r}^{\perp})=\exp\left(-\frac{1}{2}\sum_{i,j=1}^{A_P}B_{ij}\boldsymbol{r}_i^{\perp}\cdot\boldsymbol{r}_j^{\perp}+\sum_{i=1}^{A_P}u_i\boldsymbol{b}\cdot\boldsymbol{r}_i^{\perp}\right), \tag{A2}$$

where an $A_P\times A_P$ symmetric matrix B and an A_P-dimensional real vector u are given as follows:

$$B_{ij}=2\left(\lambda_i\delta_{ij}-\frac{1}{A_P}(\lambda_i+\lambda_j)+\frac{1}{A_P^2}\Lambda\right),\quad u_i=2\left(\lambda_i-\frac{1}{A_P}\Lambda\right), \tag{A3}$$

with

$$\lambda_j=\sum_{m=1}^{n}\frac{1}{2\beta_{k_m}}\delta_{ji_m},\quad \Lambda=\sum_{j=1}^{A_P}\lambda_j=\sum_{m=1}^{n}\frac{1}{2\beta_{k_m}}. \tag{A4}$$

A method of calculation of the matrix element of g is given in [10]. The elastic-scattering amplitude for NT scattering is also expressed in terms of the matrix element of g as follows:

$$F(\boldsymbol{q})=-iK\sum_{n=1}^{A_T}(-1)^n\sum_{(i_1,i_2,\ldots,i_n)}\sum_{k_1=1}^{K}\cdots\sum_{k_n=1}^{K}z_{k_1}\cdots z_{k_n}\left(\frac{1}{2\Lambda}\right)e^{-\boldsymbol{q}^2/4\Lambda}\langle\psi_0|g\left(\frac{i}{2\Lambda}u\boldsymbol{q};C,\boldsymbol{r}^{\perp}\right)|\psi_0\rangle, \tag{A5}$$

where C is an $A_P\times A_P$ matrix given by

$$C_{ij}=B_{ij}-\frac{1}{2\Lambda}u_iu_j. \tag{A6}$$

The evaluation of the matrix elements of g in Eqs. (A1) and (A5) will be aided if a normalized center-of-mass function of the projectile is introduced because then the calculation can be performed in the single-particle coordinates [10].

[1] D. L. Olson, B. L. Berman, D. E. Greiner, H. H. Heckman, P. J. Lindstrom, and H. J. Crawford, Phys. Rev. C **28**, 1602 (1983).

[2] I. Tanihata *et al.*, Phys. Rev. Lett. **55**, 2676 (1985); Phys. Lett. **160B**, 380 (1985); Phys. Lett. B **206**, 592 (1988).

[3] A. Chaumeaux, V. Layly, and R. Schaeffer, Ann. Phys. (N.Y.) **116**, 247 (1978).

[4] R. J. Glauber, in *Lectures on Theoretical Physics*, edited by W. E. Brittin and L. C. Dunham (Interscience, New York, 1959), Vol. 1, p. 315.

[5] G. F. Bertsch, H. Esbensen, and A. Sustich, Phys. Rev. C **42**, 758 (1990).

[6] Y. Ogawa, K. Yabana, and Y. Suzuki, Nucl. Phys. **A543**, 722 (1992).

[7] J. S. Al-Khalili and J. A. Tostevin, Phys. Rev. Lett. **76**, 3903 (1996); J. S. Al-Khalili, J. A. Tostevin, and I. J. Thompson, Phys. Rev. C **54**, 1843 (1996).

[8] K. Yabana, Y. Ogawa, and Y. Suzuki, Phys. Rev. C **45**, 2909 (1992).

[9] J. S. Al-Khalili, J. A. Tostevin, and J. M. Brooke, Phys. Rev. C **55**, R1018 (1997).

[10] B. Abu-Ibrahim, K. Fujimura, and Y. Suzuki, Nucl. Phys. **A657**, 391 (1999).

[11] B. Abu-Ibrahim and Y. Suzuki, Phys. Rev. C **61**, 051601(R)

(2000).
[12] N. J. DiGiacomo, R. M. DeVries, and J. C. Peng, Phys. Rev. Lett. **45**, 527 (1980); Phys. Lett. **101B**, 383 (1981).
[13] Yu. A. Berezhnoy, V. P. Mikhailyuk, and V. V. Pilipenko, J. Phys. G **18**, 85 (1992).
[14] I. Ahmad and M. A. Alvi, Phys. Rev. C **28**, 2543 (1983).
[15] T. Kobayashi *et al.*, Phys. Lett. B **232**, 51 (1989); T. Kobayashi (private communication).
[16] K. Arai, Y. Suzuki, and K. Varga, Phys. Rev. C **51**, 2488 (1995); K. Arai, Y. Suzuki, and R. G. Lovas, *ibid.* **59**, 1432 (1999).
[17] K. Varga, Y. Suzuki, and I. Tanihata, Phys. Rev. C **52**, 3013 (1995).
[18] K. Varga, Y. Suzuki, and Y. Ohbayasi, Phys. Rev. C **50**, 189 (1994).
[19] Y. Ogawa, K. Arai, Y. Suzuki, and K. Varga, Nucl. Phys. **A673**, 122 (2000).
[20] S. K. Charagi and S. K. Gupta, Phys. Rev. C **41**, 1610 (1990).
[21] V. Franco and G. K. Varma, Phys. Rev. C **15**, 1375 (1977); **18**, 349 (1978).
[22] G. S. Blanpied *et al.*, Phys. Rev. Lett. **39**, 1447 (1977).
[23] K. Varga and Y. Suzuki, Phys. Rev. C **52**, 2885 (1995).
[24] Y. Suzuki and K. Varga, *Stochastic Variational Approach to Quantum-Mechanical Few-Body Problems*, Lecture notes in physics, Vol. m54 (Springer-Verlag, Berlin, 1998).
[25] M. M. Obuti *et al.*, Nucl. Phys. **A609**, 74 (1996).
[26] A. Ozawa *et al.*, Nucl. Phys. **A608**, 63 (1996).
[27] L. Ray, Phys. Rev. C **20**, 1857 (1979).
[28] M. S. Hussein, R. A. Rego, and C. A. Bertulani, Phys. Rep. **201**, 279 (1991).
[29] K. W. Jones *et al.*, Phys. Rev. C **33**, 17 (1986).
[30] H. O. Meyer, P. Schwandt, G. L. Moake, and P. P. Singh, Phys. Rev. C **23**, 616 (1981).
[31] D. L. Olson, B. L. Berman, D. E. Greiner, H. H. Heckmann, P. J. Lindstrom, G. D. Westfall, and H. J. Crawford, Phys. Rev. C **24**, 1529 (1981).
[32] G. Fäldt, Phys. Rev. D **2**, 846 (1970).
[33] J. Formanek and R. J. Lombard, J. Phys. G **23**, 423 (1997).
[34] J. D. Jackson, *Classical Electrodynamics* (Wiley, New York, 1975).
[35] S. M. Dancoff, Phys. Rev. **72**, 1017 (1947); A. I. Akhieser and A. G. Sitenko, *ibid.* **106**, 1236 (1957).
[36] C. A. Bertulani and G. Baur, Phys. Rep. **163**, 299 (1988).
[37] A. Vitturi and F. Zardi, Phys. Rev. C **36**, 1404 (1987); S. M. Lenzi, A. Vitturi, and F. Zardi, *ibid.* **40**, 2114 (1989).
[38] A. Chaumeaux *et al.*, Nucl. Phys. **A267**, 413 (1976).
[39] J. Y. Hostachy *et al.*, Nucl. Phys. **A490**, 441 (1988).
[40] M. M. H. El-Gogary, A. S. Shalaby, and M. Y. M. Hassan, Phys. Rev. C **58**, 3513 (1998).
[41] R. C. Fuller, Phys. Rev. C **12**, 1561 (1975).
[42] S. Kox *et al.*, Phys. Rev. C **35**, 1678 (1987).